Dynamics of phosphodiester synthesis by DNA ligase

Aurélien Crut*†, Pravin A. Nair‡, Daniel A. Koster*§, Stewart Shuman‡, and Nynke H. Dekker*¶

*Kavli Institute of Nanoscience, Faculty of Applied Sciences, Delft University of Technology, Lorentzweg 1, 2628 CJ Delft, The Netherlands; and ‡Molecular Biology Program, Sloan–Kettering Institute, New York, NY 10021

Edited by Gregory A. Petsko, Brandeis University, Waltham, MA, and approved March 11, 2008 (received for review January 5, 2008)

Ligases are essential actors in DNA replication, recombination, and repair by virtue of their ability to seal breaks in the phosphodiester backbone. Ligation proceeds through a nicked DNA-adenylate intermediate (AppDNA), which must be sealed quickly to avoid creating a potentially toxic lesion. Here, we take advantage of ligase-catalyzed AMP-dependent incision of a single supercoiled DNA molecule to observe the step of phosphodiester synthesis in real time. An exponentially distributed number of supercoils was relaxed per successful incision-resealing event, from which we deduce the torque-dependent ligation probability per DNA swivel. Premature dissociation of ligase from nicked DNA-adenylate accounted for ≈10% of the observed events. The ability of ligase to form a C-shaped protein clamp around DNA is a key determinant of ligation probability per turn and the stability of the ligase-AppDNA intermediate. The estimated rate of phosphodiester synthesis by DNA ligase (400 s^{-1}) is similar to the high rates of phosphodiester synthesis by replicative DNA polymerases.

DNA ligation | DNA relaxation | magnetic tweezers

The DNA ligases are essential guardians of genome integrity. They seal 3′-OH/5′-PO_4 DNA nicks via three chemical steps (Fig. 1*a*): (*i*) ligase reacts with ATP (or NAD^+) to form a covalent ligase–adenylate intermediate, in which AMP is linked via a phosphoamide (P–N) bond to Nζ of a lysine on the enzyme; (*ii*) AMP is transferred from the ligase to the 5′-PO_4 strand at a nick to form a DNA–adenylate intermediate (AppDNA); and (*iii*) ligase catalyzes attack by the 3′-OH of the nick on AppDNA to form a phosphodiester bond and release AMP (1). Recent biochemical and crystallographic studies have illuminated the mechanism of nucleotidyl transfer, how ligases recognize nicks as "damaged," and how protein domain movements and active-site remodeling are used to choreograph the sequential steps of the ligation pathway (2, 3). In particular, the crystal structures of nick-bound ligases have revealed a conserved theme whereby ligases envelope the DNA duplex in a C-shaped protein clamp and elicit changes in DNA conformation, including bending at the nick and the adoption of A-form helical structure on the 3′-OH side of the nick (4–6).

Chlorella virus ligase (CVLig) is a minimized (298 aa) pluripotent exemplar of the ATP-dependent DNA ligase clade. It consists of an N-terminal nucleotidyltransferase domain and a C-terminal OB-fold domain. Although lacking the accessory domains found in cellular ligases, it has an intrinsic nick-sensing function and can sustain mitotic growth, excision repair, and nonhomologous end joining in budding yeast when it is the only ligase present in the cell (7–10). Accordingly, CVLig has proven to be an instructive model system for mechanistic and structural studies (11–15). For example, the atomic structure of the CVLig-AMP intermediate bound to duplex DNA with a 3′-OH/5′-PO_4 nick highlighted the key role of a β-hairpin "latch" module emanating from the OB domain in forming the C-shaped protein-DNA clamp (6) (Fig. 1*b*).

The least understood phase of nick sealing is phosphodiester bond synthesis (step 3 in Fig. 1*a*). Here, we use CVLig in the context of single-molecule nanomanipulation to directly analyze the kinetics and DNA dynamics of phosphodiester bond formation by a ligase–AppDNA complex formed *in situ* on a linear DNA. Our single-molecule experiments take advantage of the microscopic reversibility of step 3 of the ligation reaction, whereby ligase can catalyze attack of AMP on the DNA phosphodiester backbone to form a nicked DNA-adenylate. This nicked DNA-adenylate is then resealed by forward catalysis of step 3 (16). If the starting DNA substrate is a covalently closed supercoiled DNA, and if ligase releases the 3′-OH end of the AppDNA nick before executing forward step 3, the net result is incremental supercoil relaxation. AMP-dependent DNA supercoil release is a feature of many DNA ligases, including *Escherichia coli* LigA (16), T4 DNA ligase (17), vaccinia virus DNA ligase (18), and (as shown presently) *Chlorella* virus DNA ligase. This process is roughly analogous to the reactions catalyzed by type I DNA topoisomerases (TopI), except that TopI enzymes do not require AMP but instead use a tyrosine nucleophile on the enzyme to attack the phosphodiester backbone and form a covalent protein-linked DNA nick (19). The present single-molecule studies of DNA ligase provide key insights into nick sealing, especially the probability of sealing when torque is applied to a nick, the influence of protein structural elements on the stability of the ligase–AppDNA intermediate, and the rate of the chemical step of phosphodiester formation.

Results and Discussion

Ensemble and Single-Molecule Assays of Supercoil Relaxation by DNA Ligase. Purified recombinant CVLig relaxed negatively supercoiled plasmid DNA in the presence of 10 mM AMP to generate a mixture of partially relaxed topoisomers, fully relaxed circles, and nicked circular products (Fig. 1*c*). No supercoil relaxation by CVLig was detected when AMP was omitted (data not shown), indicating that the observed activity was not attributable to a contaminating topoisomerase.

In the single-molecule experiments, ≈100 plectonemic superhelical turns were introduced into a 22-kb linear duplex DNA held under constant tension by a magnetic tweezer [see *Materials and Methods*, Fig. 1*d*, and supporting information (SI) Fig. S1*a*]. Infusion of 6 nM CVLig, 5 mM $MgCl_2$, and 10 mM AMP into the reaction chamber elicited a stepwise increase in DNA extension (i.e., the distance from the surface to the magnetic bead) observable in real time (Fig. 1*d*), where each step is the result of a single cleavage-religation cycle. The simultaneous action of two enzymes has negligible probability because the delay between successive steps (typically ≈1 min; Fig. 1*d*) largely exceeds their duration (typically ≈0.1 s; see Fig. 4). The occurrence of successive cleavage/religation cycles by the same enzyme separated by a short enough pause that they appear as a single step cannot strictly be excluded, but is unlikely in view of the low specific activity of the reverse step 3 reaction. Control experiments showed that CVLig required AMP

Author contributions: A.C., S.S., and N.H.D. designed research; A.C. and P.A.N. performed research; A.C., D.A.K., S.S., and N.H.D. analyzed data; and A.C., S.S., and N.H.D. wrote the paper.

The authors declare no conflict of interest.

This article is a PNAS Direct Submission.

†Present address: Laboratoire de Spectrométrie Ionique et Moléculaire, Université Claude Bernard Lyon 1, 43 Boulevard du 11 Novembre 1918, 69622 Villeurbanne Cedex, France.

§Present address: Departments of Physics of Complex Systems and Molecular Cell Biology, Weizmann Institute of Science, Rehovot 76100, Israel.

¶To whom correspondence should be addressed. E-mail: n.h.dekker@tudelft.nl.

This article contains supporting information online at www.pnas.org/cgi/content/full/0800113105/DCSupplemental.

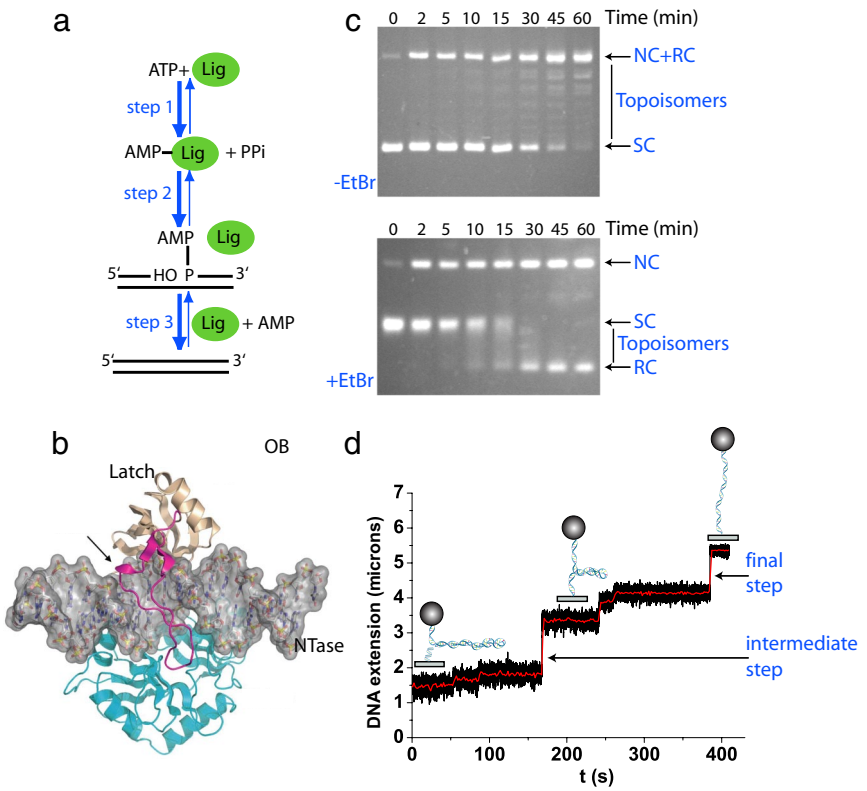

Fig. 1. CVLig and its AMP-dependent reaction reversal. (*a*) Nick sealing by DNA ligase occurs through a reaction comprising three steps: ligase adenylylation (step 1), DNA adenylylation (step 2), and phosphodiester synthesis (step 3). (*b*) The structure of CVLig bound to a nicked duplex DNA. The ligase is depicted as a ribbon trace with the nucleotidyltransferase domain in cyan, the OB domain in beige, and the latch in magenta. The DNA is rendered as a transparent surface over a stick model. The image highlights the penetration of the latch into the major grove opposite the nick and the contact between the latch and the NTase domain that closes the C-shaped ligase clamp around the DNA. (*c*) AMP-dependent relaxation of plasmid DNA in ensemble measurements. A reaction mixture (200 μl) containing 20 mM Tris·HCl (pH 8.0), 5 mM $MgCl_2$, 2 mM DTT, 0.1 mg/ml BSA, 10 mM AMP, 3 μg (1.7 pmol) supercoiled pUC19 DNA, and 1.25 μg (34 pmol) CVLig was incubated at 22°C. Aliquots (20 μl) were withdrawn at the times indicated and quenched immediately by adjustment to 0.8% SDS and 20 mM EDTA. The time 0 sample was taken before the addition of ligase. The quenched reactions were split into two 10-μl aliquots, which were analyzed in parallel by electrophoresis through horizontal 1% agarose gels containing Tris-glycine buffer (*Upper*) or Tris-glycine buffer and 0.5 μg/ml ethidium bromide (EtBr) (*Lower*). The gel in *Upper* was soaked in a 0.5 μg/ml EtBr solution for 30 min. The supercoiled (SC), relaxed circle (RC), nicked circle (NC), and partially relaxed topoisomer forms of the plasmid DNA are indicated at right. Note that because the plasmid has ≈14 negative supercoils, and the particular agarose gel system does not resolve circular DNAs with ≥7 negative supercoils (they migrate together as a single DNA band), the partially relaxed topoisomers formed by ligase at early reaction times are not apparent, although the nicked circles are. (*d*) Relaxation of a single positively supercoiled DNA molecule by CVLig in the presence of Mg^{2+} and AMP observed in real time using magnetic tweezers. The experimental approach is detailed in *Materials and Methods*. Black indicates raw data; red indicates binned data (averaged over 100 successive data points). A force of 0.5 pN was used in this experiment. One-hundred rotations were initially mechanically applied to the molecule, resulting in a highly supercoiled conformation of DNA at $t = 0$. Afterward, DNA extension increased in steps of various amplitudes as a result of CVLig activity, until the DNA was completely relaxed (t = 380 s).

to release supercoils in the single-molecule format (Fig. S2*a*) and was adept at relaxing either positively or negatively supercoiled molecules (data not shown). For subsequent experiments, we routinely used positively supercoiled DNA as it is amenable to analysis under a wider range of applied forces (Fig. S1*b*). The key feature of this assay is that it eliminates the issues of DNA-binding and prechemical conformational steps, because the DNA extension length cannot change until the nicked AppDNA complex has been formed. Therefore, the relaxation assay (described in *Materials and Methods*) monitors the fate of the DNA during single steps of phosphodiester synthesis, with precision and real-time resolution that cannot be achieved in ensemble measurements. We focused our attention on the number of supercoils released during each cycle of AMP-induced incision and AppDNA nick sealing and on the time required for a single resealing event (related to the step 3 rate constant).

Monitoring Step Sizes Yields the Ligation Probability per Turn. Our experiments demonstrate that DNA relaxation by CVLig occurs through distinct steps of nonuniform size (Fig. 2*a*). Their duration contains information on the rate of phosphodiester bond synthesis, as discussed below. The size distribution (analyzed following the approach described in *Materials and Methods*) of the "intermediate steps" (which do not result in the complete removal of plectonemes from the DNA; Fig. 1*d*) observed under a force F of 1 pN is plotted in Fig. 2*b*. "Final steps" (which do result in the complete removal of plectonemes from the DNA; Fig. 1*d*) were excluded, because their size is necessarily biased by the finite number of plectonemes present. Moreover, as discussed below, the complete relaxation of DNA during some of the final steps may result from ligase dissociation without nick sealing. The intermediate steps of supercoil relaxation by CVLig displayed an exponential size distribution at 1 pN (Fig. 2*b*). Exponential step size distributions had been observed previously for the relaxation of DNA by TopIB enzymes (20, 21), which are structurally unrelated to ligases. Such behavior signifies a DNA swiveling mechanism whereby a nicking-rejoining enzyme has a finite probability of sealing the break during any given rotation of the reactive termini past each other (20). The average step size $<\Delta Lk>$ is thereby inversely related to the probability of sealing per swivel turn. For CVLig, $<\Delta Lk> \approx 10$ at $F = 1$ pN, calculated by using a maximum-likelihood approach (22): this value corresponds to a religation probability per turn of ≈10% and is higher than the value of 2% observed for vaccinia TopIB at a similar force. CVLig maintains an exponential distribution of intermediate step sizes at forces ranging from 0.5 to 3 pN (Fig. S3). $<\Delta Lk>$ increased with greater applied force (and hence with greater applied torque; Fig. 2*b Inset* and Table 1), because the concomitant faster swiveling of DNA decreases the probability of religation per swivel turn. This dependence is well fit by simple models (red line in Fig. 2*b Inset*; for details see *SI Text* and Fig. S4).

Observation of Ligase Dissociation from Nicked DNA. Consideration of the global step size distribution (Fig. 2*a*) provided an initial clue to the occurrence of ligase dissociation. According to the probabilistic model of religation, the relaxation of large numbers of supercoils in one step leading to the complete relaxation of the DNA molecule should occur with a probability $<e^{-7} \approx 0.1\%$ when a large n value is defined as being more than seven times the average relaxation step size at the force considered. However, we observed that such large final steps occurred with a frequency of ≈10% for all of the forces tested (Table 1). This result suggested that large final steps comprised a distinct population, corresponding to linear

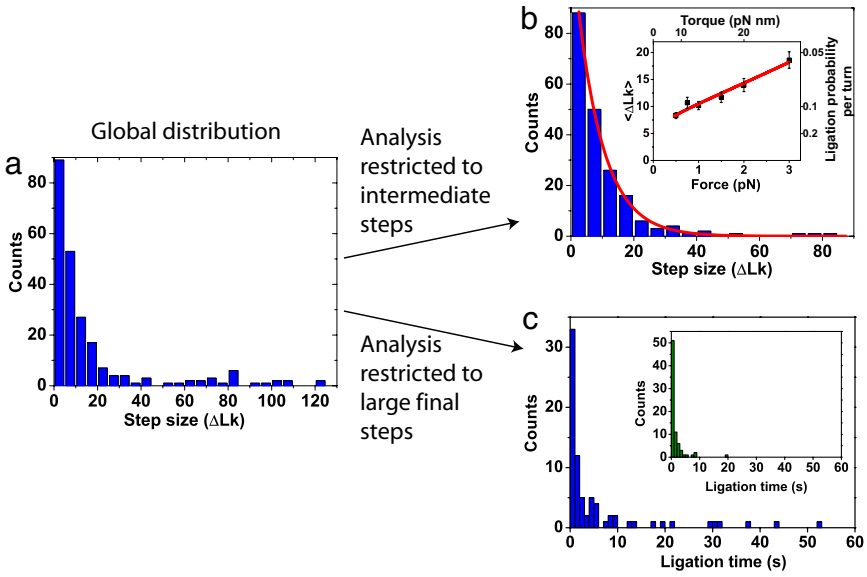

Fig. 2. Analysis of CVLig ligation probability via step size analysis. (*a*) Global distribution of step sizes observed at $F = 1$ pN. The step size ΔLk, or number n of supercoils removed, is determined from the magnitude of the DNA extension length change during each step (Fig. 1*d*) and interpolation of this value to a calibration curve of the DNA length as a function of superhelical turns applied (Fig. S1). (*b*) Distribution restricted to intermediate steps. An exponential fit of the distribution is displayed in red. (*Inset*) The dependence of the average step size (and therefore of the ligation probability per turn) on the applied force (torque) is shown. Averages and error bars were computed according to ref. 22. The experimental results were fit with a model described in *SI Text*, which describes linking number dynamics (shown in red). The optimal fitting parameters were $k_0/k_{lig} = 5$ and $\alpha = 0.2$. (*c*) Lifetime of nicked states after large final steps (77 data points). These additional experiments, described in *Materials and Methods*, demonstrate that with a 3 nM ligase concentration, DNA typically remains nicked for a few seconds after large final steps [green points; the average ligation time was 5.7 s ± 1.2 (SEM)]. The lifetime of nicked states decreased when the ligase concentration was increased to 18 nM [blue points in *Inset*; 77 data points, average 1.3 s ± 0.3 (SEM)]. Similar results for the K27A enzyme are presented in Fig. S5.

DNA molecules that had been nicked by CVLig, but not immediately sealed. These are analogous to the nicked circles formed by CVLig in the ensemble relaxation experiments (Fig. 1*c Lower*). We hypothesized that CVLig might dissociate from nicked AppDNA, in which case the sealing step would require the rebinding of ligase apoenzyme from solution to the adenylylated nick. Because ligase apoenzyme is probably a minority species in the presence of 10 mM AMP, we expected the nicked DNA-adenylates from which ligase dissociated to have a much longer half-life than the transient DNA-adenylates that were resealed by CVLig during the intermediate relaxation steps.

To test this hypothesis, we performed experiments that measured the religation time after complete relaxation of DNA, by automatically initiating magnet rotation when a threshold DNA extension was attained (see *Materials and Methods* and Fig. S5). Under constant magnet rotation, the time required to trigger plectoneme induction reflects the time it takes to seal the nick in the linear DNA molecule. The retwisting experiments revealed that DNAs that were relaxed in large final steps typically required several seconds for resealing (Fig. 2*c*), in sharp contrast with the intermediate relaxation steps in which religation occurs in $\ll$0.1 s (see dynamic analysis below). The occasional dissociation of the enzyme from nicked DNA-adenylate would neatly explain these observations. Alternatively, CVLig bound to the nicked DNA-adenylate could occasionally undergo a conformational change that prevents it from catalysis of forward step 3. Our finding that the religation time for large final steps decreased with increased ligase concentration (Fig. 2*c*) implies that ligase binding is rate-determining and thus favors the ligase-dissociation model.

Table 1. Characteristics of DNA relaxation by WT CVLig and the K27A and Δlatch mutants

Enzyme	Force, pN	Average step size ± SEM	Ligation probability per turn, %	Fraction of dissociation events
WT	0.5	8.3 ± 0.6	12	18/174 (10%)
	0.75	10.7 ± 1.0	9	13/123 (11%)
	1	10.2 ± 0.8	10	12/128 (9%)
	1.5	11.7 ± 1.0	9	10/113 (9%)
	2	14.0 ± 1.2	7	16/94 (17%)
	3	18.6 ± 1.5	5	5/60 (8%)
K27A	1	5.4 ± 0.4	19	17/204 (8%)
ΔLatch	1	43 ± 16	2	13/25 (52%)

The average step size was determined by using the maximum-likelihood approach (22). The fraction of dissociation events was defined as the fraction of steps leading to complete DNA relaxation among those starting from a configuration characterized by ΔLk greater than seven times the average step size, except for the Δlatch delete mutant, where steps leading to complete DNA relaxation among those starting from a configuration with $\Delta Lk > 100$ were considered (the previous criterion could not be used because of the large average step size for this mutant).

Our results explain the presence of nicked circle products in ensemble assays of AMP-dependent supercoil release by CVLig (Fig. 1*b*) and *E. coli* and vaccinia ligases (16, 18). Whether such dissociations occur during forward sealing of standard DNA nicks that are not under superhelical stress depends on which ligase is being studied. Several ATP-dependent bacterial ligases accumulate very high levels of AppDNA during nick sealing in the presence of ATP, reflecting a high probability of dissociation before step 3 (23, 24). Nicked DNA-adenylates are not observed during nick sealing by vaccinia ligase or CVLig, yet, DNA-adenylate does accumulate in reactions of vaccinia and CVLig when the position of the reactive 3′-OH moiety is perturbed, either by a single base-mismatch involving the 3′-OH nucleotide or by a 1-nt gap between the 3′-OH and 5′-PO_4 termini (12, 25). Similarly, T4 DNA ligase accumulates DNA-adenylate during sealing of nicks that have multiple mismatched bases on the 5′-PO_4 side of the nick (26). These findings are highly relevant to our single-molecule study of reverse step 3, insofar as the observed occasional dissociation of ligase is likely triggered by the displacement of the 3′-OH that occurs during DNA swiveling.

Supercoil Relaxation Without Ligase Adenylylation. Lys-27 is the site of covalent adenylylation in CVLig (13). The K27A mutant of CVLig (Fig. 3*a*) cannot form the covalent ligase-adenylate intermediate and hence cannot form DNA-adenylate (Fig. 1a), but K27A retains the ability to seal a preadenylylated nick (7). Because K27A cannot accept AMP from AppDNA (reverse step 2), its capacity to relax supercoils in the presence of AMP, evinced in the experiment in Fig. 3*b*, testifies that only reversal of step 3 is required for supercoil release. Similar results in ensemble relaxation had been reported for the equivalent lysine-to-alanine mutant of vaccinia DNA ligase (18). For most aspects of DNA relaxation in the

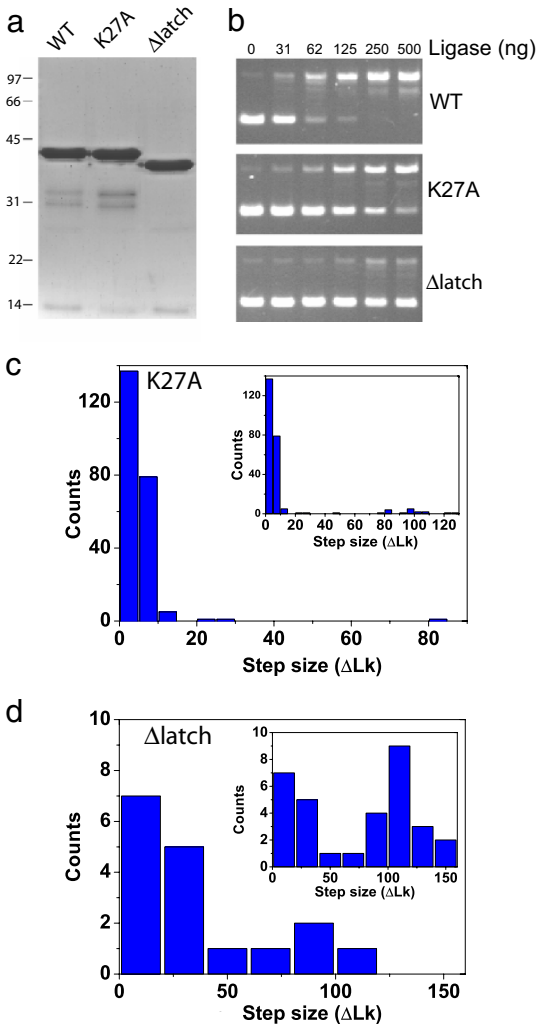

Fig. 3. Effect of K27A and Δlatch mutations on DNA relaxation and religation probability. (*a*) Aliquots (4 μg) of the phosphocellulose preparation of WT CVLig and mutants K27A and Δlatch (see *Materials and Methods*) were analyzed by SDS/PAGE. The Coomassie blue-stained gel is shown. The positions and sizes (in kDa) of marker proteins are indicated on the left. (*b*) Reaction mixtures (20 μl) containing 20 mM Tris·HCl (pH 8.0), 5 mM $MgCl_2$, 2 mM DTT, 0.1 mg/ml BSA, 10 mM AMP, 0.3 μg (170 fmol) supercoiled pUC19 DNA, and 0, 31, 62, 125, 250, and 500 ng of the indicated ligase (corresponding to 0, 0.8, 1.6, 3.4, 6.8, and 13.6 pmol of enzyme) were incubated for 60 min at 22°C. The reactions were quenched by adjustment to 0.8% SDS, 20 mM EDTA, and 5% glycerol and analyzed by electrophoresis through horizontal 1% agarose gels. (*c* and *d*) Distributions of ΔLk relaxed in intermediate steps by the K27A (*c*) and Δlatch (*d*) mutants in single-molecule experiments with $F = 1$ pN. The K27A mutant exhibits a smaller $<\Delta Lk>$ released than the WT enzyme (5.4 ± 0.4 vs. 10.2 ± 0.8; see Fig. 2*b* for comparison), corresponding to a higher religation probability per turn, whereas the Δlatch exhibited a larger $<\Delta Lk>$, corresponding to a lower religation probability per turn. (*Insets*) The overall ΔLk distributions for K27A and Δlatch including final steps are shown and highlight a large peak around $\Delta Lk = 100$, likely the result of complete relaxation in a single step, reflecting enzyme dissociation from the nicked AppDNA.

single-molecule format, K27A did not differ significantly from the WT CVLig (Fig. 3*c*, Table 1, and Fig. S6). However, the average step size $<\Delta Lk>$ at $F = 1$ pN was measurably less for K27A (5.4 ± 0.4) than for WT CVLig (10.2 ± 0.8) (Fig. 3*c Inset* and Table 1). We surmise that either a transient reversal of step 2 by WT CVLig or a conformational switch in the active site that depends on Lys-27 (13) can extend the lifetime of nicked intermediates before nick sealing, thereby allowing a larger average step size.

Role of the Latch Module and Clamp Formation. It was of particular interest to explore the role of the CVLig latch module in the dynamics of phosphodiester synthesis. The latch is disordered in the ligase apoenzyme (8, 13), but forms a β-hairpin clamp around the DNA when CVLig engages the nick (6) (Fig. 1*b*). A Δlatch mutant lacking this module (Fig. 3*a*) has reduced nick sealing activity *in vitro* and is inhibited by salt concentrations that have little impact on WT CVLig, because loss of the latch weakens binding of CVLig-AMP to nicked DNA (6). The Δlatch protein can catalyze AMP-dependent relaxation of supercoiled plasmid DNA, although with lower specific activity than CVLig or K27A (Fig. 3*b*). The salient finding from our single-molecule analysis of Δlatch was a sharp increase in the frequency of large final steps that elicit complete relaxation of the tethered linear DNA (Fig. 3*d*). This observation reflects the combination of two factors: (*i*) a 4-fold greater average step size for Δlatch, evinced by $<\Delta Lk> = 43 \pm 16$ during intermediate step events (Fig. 3*d Inset* and Table 1) and (*ii*) a higher probability of dissociation of Δlatch from nicked DNA adenylate compared with the CVLig and K27A (Fig. 3*d* and Table 1). These findings attest to the crucial role of the C-shaped protein clamp in stabilizing the ligase-AppDNA intermediate.

The Rate of Phosphodiester Synthesis. Finally, the single-molecule analysis provides an otherwise unattainable estimate of the rate of phosphodiester synthesis during the ligation reaction. CVLig and many other ligases do not generate detectable levels of the App-DNA intermediate during a single-turnover nick sealing reaction, because the rate of phosphodiester synthesis (step 3) is much faster than the rate of DNA-adenylate formation (step 2). Although step 3 can be studied in isolation by reacting the ligase apoenzyme with a preadenylylated nicked duplex in the absence of ATP, the observed rates of single-turnover AppDNA sealing (≈0.05 s^{-1} for CVLig) are paradoxically much slower than the rate of the composite 3′-OH/5′-PO_4 nick sealing reaction (≥0.5 s^{-1} for CVLig) (12). To explain this oddity, while defending the clearly established intermediacy of DNA-adenylate, it was postulated that the reaction of ligase apoenzyme with AppDNA in solution is subject to rate-limiting binding or conformational steps that do not apply when AppDNA is formed *in situ* by ligase-adenylate bound at a nick (12, 27).

We find here that DNA extension during an intermediate step triggered by CVLig is typically achieved within 0.1 s at $F = 0.5$ pN (Fig. 4*a*). Because an intermediate plateau in the DNA extension indicates a complete absence of nicks in the DNA, it follows that the rate of phosphodiester bond synthesis (k_{lig}) exceeds 10 s^{-1}. However, a quantitative description of DNA extension dynamics during stepwise relaxation allows us to significantly refine this bound. In particular, we observed that the dynamics of DNA extension during ligase-mediated relaxation were very similar to the dynamics of bare DNA. For instance, >80% of the intermediate steps observed under $F = 0.5$ pN were accurately described by the quasistatic model used in ref. 28 (Fig. 4*a* and *SI Text*), which takes into account the magnetic force, the drag opposing the motion of the bead linked to DNA, and the tension in the DNA, where for the latter we assume the equilibrium force-extension relation at the degree of supercoiling present in the DNA at the end of the relaxation. This accurate description implies that supercoil removal by CVLig occurs on faster time scales than DNA extension, as in the case of enzyme-independent supercoil removal (28). The description of the dynamics of intermediate steps by this model further implies that nick sealing occurs at a rate of the order or higher than the acquisition rate in our experiments, 60 s^{-1} (Fig. 4*a*). As this is a lower bound to even the lowest rates of nick sealing by CVLig, corresponding the largest ΔLk removed (e.g., Fig. 4*a*, which involves the removal of ≈50 supercoils), the average ligation rate k_{lig} should be even higher. Assuming that the ligation time in a single cleavage-religation event is proportional to the number of supercoils released, and using $<\Delta Lk> = 8.3$ at $F = 0.5$ pN (Fig. 2*b*), the lower

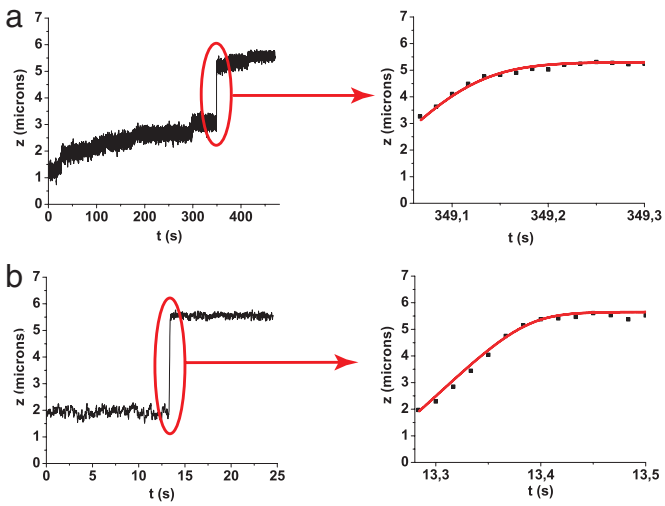

Fig. 4. Rate of CVLig phosphodiester synthesis probed via supercoil relaxation dynamics. Both examples shown are representative traces obtained at $F = 0.5$ pN. (*a*) Analysis of a large step leading to incomplete DNA relaxation ($\Delta Lk = +30$ at the end of the step). The dynamics resulting from the quasistatic model for supercoiled DNA (using the force-extension behavior measured at $\Delta Lk = +30$) are shown in red for comparison. (*b*) Analysis of a large step leading to complete DNA relaxation. The experimental results are shown in black. The dynamics resulting from the quasistatic model for torsionally relaxed DNA are shown in red. The quasistatic model was accurate for >80% of the traces, both for intermediate and final steps.

bound estimate for k_{lig} increases (50/8.3≈6-fold) to ≈400 s^{-1}. The dynamics of final relaxation steps are also described by a quasistatic model for torsionally relaxed DNA (in >80% of the events observed at $F = 0.5$ pN; Fig. 4*b*), which is fully expected given their attribution to ligase dissociation events, as described above.

Comparison to DNA Topoisomerase. Our work generalizes the torque-dependent religation mechanism observed for TopIs to a novel category of enzymes, DNA ligases. However, it is also noteworthy that certain features of AMP-induced relaxation by CVLig differ from those of DNA relaxation by TopIB enzymes, despite the fact that both enzymes engage duplex DNA as a C-shaped protein clamp (29, 30). As we have seen, the ligase clamp does not impose observable friction during DNA swiveling, but the TopIB clamp does (20, 21). Although the ligation probabilities per swivel turn P_{lig} differ only by a factor of five between CVLig and TopIB (10% and 2% at $F = 1$ pN, respectively), differing interaction times T_{res} between the rotating DNA strands could nonetheless imply quite different religation rates, because the ligation probability is equal to the product of the religation rate and the interaction time, $P_{lig} = k_{lig}T_{res}$ (*SI Text*). The dynamical analysis described above also yields a lower bound (10 s^{-1}) for the rate of religation by the covalent TopIB-DNA intermediate in a single-molecule format, which is much slower than the $k_{lig} > 400$ s^{-1} observed for phosphodiester synthesis by the ligase–AppDNA complex. However, if the increased friction observed for TopIB is attributable to the presence of multiple energy barriers, then the corresponding estimate of T_{res} (and hence k_{lig}) may be less precise (20).

Analogy to DNA Polymerases. Ligase-mediated synthesis of a 3′-5′ DNA phosphodiester by attack of a DNA 3-OH end on the activated 5′ head group of the AppDNA strand with displacement of AMP is chemically analogous to phosphodiester synthesis by DNA polymerase, which entails attack of a primer 3′-OH on a dNTP with expulsion of pyrophosphate. Indeed, it is remarkable that the estimated rate of phosphodiester synthesis by CVLig (≈400 s^{-1}) is similar to the rates of phosphodiester synthesis by a fast-moving replicative DNA polymerase (≈800 s^{-1}) (31). It is critical that replicative DNA polymerases avoid dissociating prematurely from the replication fork; in the same vein, it is desirable that DNA ligases not dissociate prematurely from the AppDNA intermediate. Free AppDNA ends would be difficult to reseal directly, given that: (*i*) ligases are predominantly in the adenylylated state at physiological ATP concentrations; and (*ii*) ligase-adenylate can neither seal nor deadenylate an AppDNA terminus. Our studies show that the DNA clamp-forming latch module of CVLig helps stabilize the ligase-AppDNA intermediate. Nonetheless, the WT ligase does dissociate prematurely in a minority of events when the DNA is driven to swivel about the nick. Although it is not known how often ligase acts as a relaxing enzyme in living cells, mechanisms do exist to deal with nicked DNA-adenylates when they arise. Eukarya resolve this roadblock to DNA repair via the action of aprataxin, an enzyme that specifically hydrolyzes the AMP from AppDNA to restore a ligatable 5′-PO_4 end (32).

Materials and Methods

Ligase Purification. Large-scale purifications of WT CVLig and the K27A mutant from soluble bacterial lysates were performed as described (6). Small-scale purifications of WT CVLig, K27A, and the Δlatch mutant from lysates of 100-ml cultures of isopropyl β-D-thiogalactoside-induced *E. coli* BL21(DE3)/pET-His_{10}-CVLig cells were achieved by sequential Ni-agarose and phosphocellulose chromatography steps. Protein concentrations were determined by using the BioRad dye reagent with BSA as a standard. The polypeptide compositions of the ligase preparations were analyzed by SDS/PAGE (Fig. 3*a*).

Magnetic Tweezers Experimental Configuration. Magnetic tweezers used a pair of magnets to control both the tension and the linking number of a single linear dsDNA molecule anchored to a functionalized glass surface on one side and attached to a magnetic bead on the other side (Fig. S1*a*). The upward magnetic stretching force F applied to the DNA was generated by means of a pair of magnets positioned above the sample. The amplitude of F was modified by the vertical translation of the magnets. The linking number of the molecule was controlled by the rotation of the magnets about the z axis. The 3D position of the bead was tracked in real time at 60 Hz. In particular, the vertical position z of the bead (i.e., the end-to-end DNA extension) was determined from the analysis of its diffraction pattern, with an accuracy of ≈10 nm. Additionally, beads fixed to the glass surface were used as references to correct for mechanical drift. The DNA constructs used in the magnetic tweezers were prepared by ligating both ends of 20.7-kb DNA molecules to 0.6-kb-long PCR fragments containing multiple biotin and digoxigenin groups, respectively. The DNA molecules were then incubated with streptavidin-functionalized magnetic beads (Myone; Dynal). Experiments were performed in flow cells functionalized with polystyrene [1% (wt/vol) in toluene], antidigoxigenin (50 μg/ml in PBS), and finally polyglutamic acid (10 mg/ml in PBS), where the latter step reduced nonspecific interactions.

Calibrations Performed in the Magnetic Tweezers. Calibrations were performed for each magnetically captured DNA-tethered bead (DNA-bead) in relaxation assay buffer before performing the experiments involving ligase. These calibrations ensure that: (*i*) The magnetic bead under study is connected to the surface via a single, unnicked DNA molecule; (*ii*) potential offsets of ΔLk are corrected; (*iii*) the dependence of the force F on the vertical position of the magnets is precisely determined; (*iv*) the contour length and the persistence length of the molecule under study are known; (*v*) the sizes of plectonemes formed under various forces are determined; and (*vi*) the dynamic analysis of intermediate steps in the single-molecule relaxation assay can be performed.

Calibrations *i* and *ii* were achieved by investigating the response of the DNA-bead under study when magnets were rotated. An asymmetrical response to magnet rotation under forces of ≈1 pN, like the one displayed in Fig. S1*b*, constitutes a signature of the attachment of a single coilable DNA molecule between the bead and the surface and contrasts with the symmetrical response observed when two or more DNA molecules are attached between the surface and the magnetic bead wrap around each other (33, 34). Additionally, the symmetrical rotation observed at lower forces (the example of 0.5 pN is displayed in Fig. S1*b*) allows for the precise determination of the number of magnet rotations corresponding to $\Delta Lk = 0$. Calibrations *iii* and *iv* were achieved by recording the Brownian motion of the bead for various vertical positions of the magnet pair. The force F for each of these positions was deduced from the analysis of the lateral fluctuations of the bead. Then, the dependence of the molecule average extension on force was fitted to the worm-like-chain model,

which gives access to its contour and persistence lengths. Calibration *v* was realized by measuring the DNA extension (averaged over 512 successive frames) at a given force for various values of ΔLk. The linear dependence of this extension with ΔLk in the plectonemic regime (Fig. S1*b*) allows for the subsequent conversion between DNA extension and ΔLk in the analysis of relaxation experiments. Finally, calibration *vi* was performed to permit the dynamic analysis of intermediate steps. This calibration recorded the force-extension behavior of DNA for a large number of ΔLk values. (Fig. S1*c*).

Relaxation Assays in the Magnetic Tweezers. Unless otherwise noted, the buffer used for the DNA relaxation assays in the single-molecule experiments included 20 mM Tris (pH 7.8), 5 mM $MgCl_2$, 2 mM DTT, 0.1 mg/ml BSA, and 10 mM AMP. This buffer was passed through a 0.22-μm filter unit before use. WT and K27A enzymes were used at 6 nM and the Δlatch mutant was used at 12 nM. Experiments started by inducing positive plectonemes along DNA via magnet rotation. Enzymes were regularly reflushed at the same concentration to avoid a drop in activity. No activity was observed in negative controls lacking either AMP, CVLig, or magnesium (Fig. S2*a*), indicating that the stepwise reaction observed when all these components are present is attributable to AMP- and magnesium-dependent DNA relaxation by CVLig. In the context of the study of DNA relaxation induced by CVLig, it is important to verify that the stepwise behavior is caused by successive nicking/religation events induced by the enzyme rather than by other factors, in particular by sticking/unsticking of DNA fragments to the surface (possibly induced by the presence of proteins along DNA). Experimentally, the occurrence of this problem can be addressed by monitoring the response of a supercoiled DNA molecule to a rapid translation of the magnets inducing a large modification of the force applied to the molecule. Relaxation experiments were performed only while the DNA molecule under study exhibited a fast, step-free response such as the one represented in Fig. S2*b*.

Measurement of the Lifetime of Nicked States After Large Final Steps. We describe how one can measure the time during which DNA remains nicked after a large final step. This measurement was accomplished by exploiting the different response of nicked and supercoiled DNA molecules to magnet rotation. In our experiments, we triggered continuous magnet rotation when relaxation of supercoiled DNA resulted in an extension above a given threshold. Rotation was continued until the DNA extension was again reduced to values below the threshold as a consequence of supercoil induction (Fig. S5). Final steps can be identified as events that temporarily increase the DNA extension to that of relaxed level. As example, the event presented in Fig. S5*a* meets this criterion. A low threshold was used to ensure the selection of large final steps (horizontal green lines in Fig. S5). For such events, continuous magnet rotation after DNA relaxation systematically results in a plateau in the DNA extension, the duration of which ranges from ≈2 s to several tens of seconds. The times t_{nick} and $t_{sealing}$, corresponding to the successive creation and sealing of a nick by CVLig, are deduced from these traces. t_{nick} is easily determined, because it coincides with a sudden increase of DNA extension. Twisting an initially relaxed DNA molecule does not affect its extension until the buckling transition is reached; thus, a ''buckling time'' $t_{buckling}$ (typically 2 s under a 1-pN force with magnets rotating at 20 Hz) has to be substracted from the time at which the plateau ends to get a reliable estimation of $t_{sealing}$ (35). We define $t_{ligation}$, the lifetime of the nicked intermediates in the ligation reaction, as $t_{ligation} = t_{sealing} - t_{buckling} - t_{nick}$.

Step-Fitting Procedure. Experimental traces were analyzed by using the step-finding algorithm developed by Kerssemakers *et al.* (36), which assumes a Gaussian-distributed noise but makes no *a priori* assumptions regarding either the step size or the dwell time. The results were compared with a separated fitting routine based on the computation of the standard deviation of the DNA extension over a user-defined time range around each data point. Both algorithms yielded very similar distributions, demonstrating that these distributions were not influenced by the particular step-fitting routine used. Final steps were not included in the distribution to determine the average step size as they introduce artifacts. To correct for the resulting selection bias in the distribution, a maximum-likelihood approach was used (22).

ACKNOWLEDGMENTS. We thank Armin Rasidovic and Xiaomin Hao for help with the single-molecule experiments; Jan Lipfert for useful discussions; Susanne Hage for preparing the DNA constructs; Jacob Kerssemakers and Irene Dujovne for input on the step-fitting algorithms; and Richard A. Neher and Ulrich Gerland for pointing out the formal requirement for inclusion of the reverse torque in the derivation of the step size in the supporting information. This work was supported by grants from the Foundation for Fundamental Research on Matter and The Netherlands Organization for Scientific Research (to N.H.D.) and by National Institutes of Health Grant GM63611 (to S.S.). S.S. is an American Cancer Society Research Professor.

1. Lehman IR (1974) DNA ligase: Structure, mechanism, and function. *Science* 186:790–797.
2. Shuman S, Lima CD (2004) The polynucleotide ligase and RNA capping enzyme superfamily of covalent nucleotidyltransferases. *Curr Opin Struct Biol* 14:757–764.
3. Tomkinson AE, Vijayakumar S, Pascal JM, Ellenberger T (2006) DNA ligases: Structure, reaction mechanism, and function. *Chem Rev* 106:687–699.
4. Pascal JM, O'Brien PJ, Tomkinson AE, Ellenberger T (2004) Human DNA ligase I completely encircles and partially unwinds nicked DNA. *Nature* 432:473–478.
5. Nandakumar J, Nair PA, Shuman S (2007) Last stop on the road to repair: Structure of *E. coli* DNA ligase bound to nicked DNA adenylate. *Mol Cell* 26:257–271.
6. Nair PA, *et al.* (2007) Structural basis for nick recognition by a minimal pluripotent DNA ligase. *Nat Struct Mol Biol* 14:770–778.
7. Sriskanda V, Shuman S (1998) *Chlorella* virus DNA ligase: Nick recognition and mutational analysis. *Nucleic Acids Res* 26:525–531.
8. Odell M, Shuman S (1999) Footprinting of *Chlorella* virus DNA ligase bound at a nick in duplex DNA. *J Biol Chem* 274:14032–14039.
9. Sriskanda V, Schwer B, Ho CK, Shuman S (1999) Mutational analysis of *Escherichia coli* DNA ligase identifies amino acids required for nick ligation *in vitro* and for *in vivo* complementation of the growth of yeast cells deleted for CDC9 and LIG4. *Nucleic Acids Res* 27:3953–3963.
10. Odell M, Malinina L, Sriskanda V, Teplova M, Shuman S (2003) Analysis of the DNA joining repertoire of *Chlorella* virus DNA ligase and a new crystal structure of the ligase-adenylate intermediate. *Nucleic Acids Res* 31:5090–5100.
11. Sriskanda V, Shuman S (1998) Specificity and fidelity of strand joining by *Chlorella* virus DNA ligase. *Nucleic Acids Res* 26:3536–3541.
12. Sriskanda V, Shuman S (1998) Mutational analysis of *Chlorella* virus DNA ligase: Catalytic roles of domain I and motif VI. *Nucleic Acids Res* 26:4618–4625.
13. Odell M, Sriskanda V, Shuman S, Nikolov DB (2000) Crystal structure of eukaryotic DNA ligase-adenylate illuminates the mechanism of nick sensing and strand joining. *Mol Cell* 6:1183–1193.
14. Sriskanda V, Shuman S (2002) Role of nucleotidyltransferase motifs I, III, and IV in the catalysis of phosphodiester bond formation by *Chlorella* virus DNA ligase. *Nucleic Acids Res* 30:903–911.
15. Sriskanda V, Shuman S (2002) Role of nucleotidyl transferase motif V in strand joining by *Chlorella* virus DNA ligase. *J Biol Chem* 277:9661–9667.
16. Modrich P, Lehman IR, Wang JC (1972) Enzymatic joining of polynucleotides. XI. Reversal of *Escherichia coli* deoxyribonucleic acid ligase reaction. *J Biol Chem* 247:6370–6372.
17. Montecucco A, Ciarrocchi G (1988) AMP-dependent DNA relaxation catalyzed by DNA ligase occurs by a nicking-closing mechanism. *Nucleic Acids Res* 16:7369–7381.
18. Sekiguchi J, Shuman S (1997) Nick sensing by vaccinia virus DNA ligase requires a 5′ phosphate at the nick and occupancy of the adenylate binding site on the enzyme. *J Virol* 71:9679–9684.
19. Corbett KD, Berger JM (2004) Structure, molecular mechanisms, and evolutionary relationships in DNA topoisomerases. *Annu Rev Biophys Biomol Struct* 33:95–118.
20. Koster DA, Croquette V, Dekker C, Shuman S, Dekker NH (2005) Friction and torque govern the relaxation of DNA supercoils by eukaryotic topoisomerase IB. *Nature* 434:671–674.
21. Taneja B, Schnurr B, Slesarev A, Marko JF, Mondragon A (2007) Topoisomerase V relaxes supercoiled DNA by a constrained swiveling mechanism. *Proc Natl Acad Sci USA* 104:14670–14675.
22. Koster DA, Wiggins CH, Dekker NH (2006) Multiple events on single molecules: Unbiased estimation in single-molecule biophysics. *Proc Natl Acad Sci USA* 103:1750–1755.
23. Gong C, Martins A, Bongiorno P, Glickman M, Shuman S (2004) Biochemical and genetic analysis of the four DNA ligases of mycobacteria. *J Biol Chem* 279:20594–20606.
24. Zhu H, Shuman S (2007) Characterization of *Agrobacterium tumefaciens* DNA ligases C and D. *Nucleic Acids Res* 35:3631–3645.
25. Shuman S (1995) *Vaccinia* virus DNA ligase: Specificity, fidelity, and inhibition. *Biochemistry* 34:16138–16147.
26. Cherepanov AV, de Vries S (2003) Kinetics and thermodynamics of nick sealing by T4 DNA ligase. *Eur J Biochem* 270:4315–4325.
27. Modrich P, Lehman IR (1973) Deoxyribonucleic acid ligase: A steady-state kinetic analysis of the reaction catalyzed by the enzyme from *Escherichia coli*. *J Biol Chem* 248:7502–7511.
28. Crut A, Koster DA, Seidel R, Wiggins CH, Dekker NH (2007) Fast dynamics of supercoiled DNA revealed by single-molecule experiments. *Proc Natl Acad Sci USA* 104:11957–11962.
29. Redinbo MR, Stewart L, Kuhn P, Champoux JJ, Hol WG (1998) Crystal structures of human topoisomerase I in covalent and noncovalent complexes with DNA. *Science* 279:1504–1513.
30. Perry K, Hwang Y, Bushman FD, Van Duyne GD (2006) Structural basis for specificity in the poxvirus topoisomerase. *Mol Cell* 23:343–354.
31. Mok M, Marians KJ (1987) The *Escherichia coli* preprimosome and DNA B helicase can form replication forks that move at the same rate. *J Biol Chem* 262:16644–16654.
32. Ahel I, *et al.* (2006) The neurodegenerative disease protein aprataxin resolves abortive DNA ligation intermediates. *Nature* 443:713–716.
33. Charvin G, Vologodskii A, Bensimon D, Croquette V (2005) Braiding DNA: Experiments, simulations, and models. *Biophys J* 88:4124–4136.
34. Stone MD, *et al.* (2003) Chirality sensing by Escherichia coli topoisomerase IV and the mechanism of type II topoisomerases. *Proc Natl Acad Sci USA* 100:8654–8659.
35. Koster DA, Palle K, Bot ES, Bjornsti MA, Dekker NH (2007) Antitumour drugs impede DNA uncoiling by topoisomerase I. *Nature* 448:213–217.
36. Kerssemakers JW, *et al.* (2006) Assembly dynamics of microtubules at molecular resolution. *Nature* 442:709–712.